Received 7 April 2016; revised 2 June 2016; accepted 8 June 2016. Date of publication 10 June 2016; date of current version 24 October 2016.
The review of this paper was arranged by Editor M. Chan.

Digital Object Identifier 10.1109/JEDS.2016.2579880

Magnetically Tuned Varistor and Its Embedded Transistors

RAGHVENDRA K. PANDEY[1] (Life Senior Member, IEEE), WILLIAM A. STAPLETON[1] (Member, IEEE), AND RAINER SCHAD[2]

1 Ingram School of Engineering, Texas State University, San Marcos, TX 78666, USA
2 Department of Physics, University of Alabama, Tuscaloosa, AL 35487, USA

CORRESPONDING AUTHOR: R. K. PANDEY (e-mail: mailto:rkpandey@att.net)

This work was supported by the National Science Foundation under Grant ECCS-1025395 and Grant DMR-0213985.

ABSTRACT This paper describes the properties and potential applications of a hybrid device consisting of a varistor diode and its embedded transistor whose origin lies in a magnetically tuned varistor diode. It is shown how the output current (or voltage) of a varistor based on a magnetic oxide semiconductor can be manipulated by the application of a magnetic field to produce an embedded device with characteristics similar to that of a conventional transistor. Following the tradition of microelectronics, we name it the HFET transistor where H stands for a magnetic field. Two types of embedded HFET devices are described here; one with the current–voltage (I–V) characteristics and the other with voltage–current (V–I) characteristics. Both I–V and V–I devices exhibit high degree of nonlinearly but only in the V–I mode of the HFET device well-developed saturation regions of output signals are found. The room temperature HFET in its V–I mode appears to be also a good electronic switch with well-defined "off" and "on" states. Saturated regions of output signals and electronic switching are the signature property of these HFET transistors along with the capacity of providing a good level of signal amplification. When cooled to 100 K the HFET V-I device appears to lose partially the electronic switching property but gain in signal amplifying potential. The HFET device in I–V mode does not display the defining properties of electronic switching but can amplify signals by almost 400%.

INDEX TERMS Varistors, transistors, HFET, MAGFET, spin transistors.

I. INTRODUCTION

The subject of this paper is a magnetically induced dual purpose hybrid device which can be processed on a single substrate and can be used either as a magnetically tuned varistor or as a magnetically induced transistor. Two types of hybrid devices are discussed. The first device evolves when the current-voltage (I-V) characteristics of a varistor is magnetically tuned; and the second when the voltage-current (V-I) characteristics of the IH varistor is manipulated by applying magnetic fields at room temperature and then at 100K. In each of these three cases the resulting devices serve as magnetically tuned varistors with the acquired property of signal amplification. Once the contributions of magnetic field is separated from the output current (or, voltage) of the varistor we come upon an embedded device with typical characteristics of a transistor. We therefore label this device as HFET which stands for *magnetically tuned field effect transistor* in analogy to the well-established field effect transistor with the acronym of FET. The difference between a FET and an HFET is that in a FET the field is the electric field while in an HFET the field is magnetic with the symbol of H. We believe our device may be considered as a new addition to the field of magnetic transistors.

The history of magnetic transistors is long and interesting. It was in 1959 that the MOS transistor (metal-oxide semiconductor transistor) was discovered in Bell Labs [1]. The device achieved almost instant success as a field-effect amplifier. The race for a magnetic transistor began and the first successful device was discovered in 1966 at Westinghouse Electric Corporation [2]. Using a silicon sample the inventors showed the dependence of Hall voltage both on drain

current and gate voltage. The device also exhibited transistor like I-V curves that was dependent upon gate voltages. It was the first magnetic field-effect transistor based on the MOS configuration. Unfortunately the magnetic transistor never got the importance and name recognition that of a semiconductor transistor. Since the device was slow and did not solve any of the pressing needs of telephone technology at the time it was soon abandoned. However, the quest for an efficient magnetic transistor continued. Then in 1971 a split-drain MOS structure was invented that could successfully measure the differential Hall voltages [3]. The device came to be known as MAGFET which stands for *magnetic field effect transistor.*

It would take another twenty years between the discovery of MAGFET and the emergence of a new class of magnetic transistors. In 1990 the first spintronic transistor was reported which is also known as spin-mediated transistor. This spintronic device bears resemblance to conventional semiconductor transistors. It is based on a configuration similar to that of a typical MOSFET(metal-oxide-semiconductor field-effect-transistor) [4]. The current modulation is achieved by the mechanism of spin precession arising from the spin-orbit coupling in a substrate of indium gallium arsenide (InGaAs) which is a narrow bandgap semiconductor. Instead of a gate oxide a layer of indium aluminum arsenide (InAlAs) is integrated with the InGaAs substrate. For metallic contacts ferromagnetic iron, which acts as the reservoir for magnetic spins ($\pm\frac{1}{2} \approx \uparrow$ or $\downarrow$ polarized states), is used as source (S) and drain (D) while the gate (G) contact is a Schottky contact.

Soon after the discovery of spin-mediated transistor another spintronic device was reported in 1995 which is based on the spin-valve effect that can be monitored in the multilayers of giant magnetoresistive materials. This device uses a configuration similar to that commonly used in a bipolar junction transistor (BJT). The transmission characteristics of the spin-dependent transport exhibit well defined saturation regions similar to the current (I) and voltage (V) characteristics of a conventional transistor [5].

The distinction between our HFET and other magnetic transistors is subtle; the most important being that the HFETs are based on very simple platforms and equally simple physics whereas the typical magnetic transistors described above are based on highly sophisticated physics and produced on configurations that are not trivial to produce.

II. SUBSTRATE MATERIAL AND ITS PROCESSING

A. CHEMICAL AND PHYSICAL NATURE OF SUBSTRATE MATERIAL

Varistors built on IHC 45 ceramic substrates are the basis for producing magnetically induced hybrid devices. IHC 45 is the combination of 55 atomic % ilmenite ($FeTiO_3$) and 45 atomic % hematite (Fe_2O_3). Polycrystalline IHC45 was chosen as the substrate material because of its interesting semiconducting and magnetic properties. It is an important member of the iron titanate oxide semiconductor group which was discovered around 1957 [6], [7]. Depending upon the concentration of hematite (x) in ilmenite the members of the solid solution series can be either of n-type or p-type, and magnetic or nonmagnetic. The transition between n-type and p-type occurs around when $x \approx 0.2$. Some of its physical properties relevant to our interest are given in Table 1.

TABLE 1. Selected physical properties of IHC45.

Curie Point, T_C (K)	Resistivity, ρ (Ω·cm)	Seebeck coefficient, S (μV/K)	Polarity/electron mobility μ (cm^2/Vs)	Bandgap, E_g (eV)	Carrier concentration, n_e (per cm^3)	Radiation hardness
610	2.38	160	p-type/0.31	2.28 (indirect)	$10^{19\text{-}21}$	excellent

Because of its relatively high magnetic Curie temperature, wide bandgap, and excellent hardness to radiation IHC45 is found to be an attractive substrate material for high temperature magnetic and electronic applications. The devices built on IHC 45 substrate could also be of interest to space electronics, and defense electronics.

B. CERAMIC PROCESSING AND SURFACE CHARACTERIZATIONS OF IHC45

High density bulk ceramic samples were processed using the standard steps of ball milling, sintering, pressing at high pressures, and finally annealing at high temperatures in air [8]. The quality, crystal structure, surface integrity and over all integrity of the ceramic samples produced were ascertained by subjecting them to a number of analyses commonly done in the field of materials science. These experiments included x-ray diffraction (XRD), scanning electron microscopy (SEM) and energy dispersive x-ray analysis (EDAX). The results confirmed their high quality.

Initially the resistance of the as-processed ceramic sample was high and not suitable for noiseless I-V measurements. After extensive annealing in argon and partial vacuum the resistance decreased and was now in the range of 3-5 kΩ, making the sample acceptable for electrical measurements. Originally the IHC45 ceramic samples were found to be of n-type polarity but after being annealed in flowing argon at about 1100 °C for number of hours the polarity switched to p-type. It is not unusual that in ceramic oxide semiconductors polarity can switch from n-type to p-type and vice versa after extensive annealing at high temperatures in the presence of specialized atmospheres. Annealing can induce minor changes in sample's chemical composition leading to polarity switching. Annealing also affects such fundamental properties as donor density, density of states, and barrier heights [9], [10].

Annealing is a very important step that must be carefully executed in ceramic processing because it enhances the homogeneity of samples while simultaneously allowing grains (G) to grow bigger in size and grain boundaries (GB) to develop fully. In a ceramic sample, grain boundaries

are sandwiched between two neighboring grains forming a G-GB-G structure through which the current transport must proceed uninterrupted. The internal configuration of a varistor consists of a large number of G-GB-G structures. It is obvious that for a superior performance of a varistor diode the G-GB-G structures must be well developed with as few defects as possible.

III. MAGNETIC TUNING OF I-V CHARACTERISTICS OF AN IHC45 VARISTOR

A. SAMPLE PREPARATION

Samples for studying the current-voltage (I-V) characteristics of IHC45 were cut as small square pieces having the dimensions of approximately 4 mm x 4 mm x 1.5 mm. They were polished to a high shine and then examined under an optical microscope to assure that they were free of any micro cracks and other surface defects. Two dot contacts using a conductive silver epoxy were affixed 1 mm apart on the upper polished surface and allowed to air dry. Then they were annealed at approximately 250 °C for 30-45 minutes. This allowed the silver contacts to bind strongly with the substrates and organic epoxy to burn off.

B. EXPERIMENTAL SET UP FOR DATA COLLECTION

The experimental set up of Figure 1 was used for magnetic tuning of the varistor [11]. It is similar to the configuration of the Hall effect experiment which is universally used for determining the mobility and carrier concentration of a semiconductor material. The samples were mounted on the test fixture of a precision semiconductor parametric analyzer (HP-4145 B, Hewlett Packard Company, Palo Alto, CA) using fine silver wires.

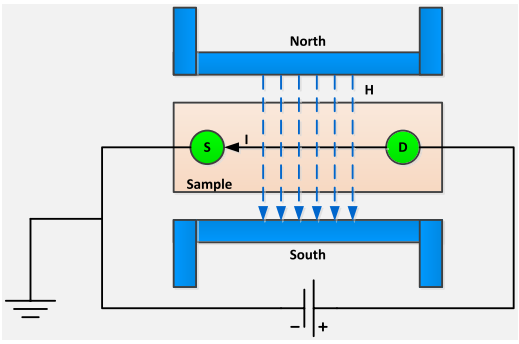

FIGURE 1. Experimental setup for determining the varistor response to an applied magnetic field, H. The H-field is perpendicular to the electric current, I, between source (S) and drain (D) [11].

The test fixture was covered during data collection to keep the sample in dark in order to avoid generation of photocurrents and any other interference from light source that could possibly corrupt the actual data produced by the varistor. Silver was chosen as a contact metal because it has been found to produce depletion regions at the interface of IHC 45 leading to the formation of a potential barrier that enables the current to be rectifying in nature [12].

The samples were oriented such that the current (I) flowing from D (drain) to S (source) contacts was perpendicular to the applied magnetic field (H). The H-field was varied gradually in steps of 500 G for the range of 0<H<4500G. After allowing the system to come to an equilibrium the data were collected. The difference between our experiment and the Hall effect experiment is subtle. We monitor the change in current induced by the application of a magnetic field instead of monitoring the Hall voltage that develops along a direction which is perpendicular simultaneously to the directions of the current (I) and magnetic field (H), respectively.

The first I-V plot that was generated with H = 0 G is the intrinsic characteristics of the varistor. The drain voltage, V_d, was swept for the range of ±5V in steps of approximately 80 mV which produced a large set of data points that could be used for analysis to reach a reliable conclusion. Subsequent to that the sample was exposed to magnetic fields to record the field modified drain current. For the V-I experiments also current was applied in small steps between the source and drain and the resulting voltage monitored. Three sets of experiments were done: (1) to determine the magnetic field dependence of the I-V characteristics of the varistor at room temperature; (2) to determine the magnetic field induced changes in the V-I characteristics of the device also at room temperature; and (3) reparation of the second experiments while cooling the sample to 100K.

IV. RESULTS AND DISCUSSION

A. EXPERIMENT 1: MAGNETIC FIELD DEPENDENCE OF I-V CHARACTERISTICS OF AN IHC45 VARISTOR AT ROOM TEMPERATURE

The current-voltage characteristics of the varistor as a function of magnetic field, H, are plotted Figure 2. The current increases conspicuously as soon as a magnetic field of 500 G is applied. Subsequent to that the increase in current takes place in smaller units so that the individual I-V plots begin to cluster making it difficult to distinguish them from each other. Therefore, for clarity we show only four I-V plots corresponding to H = 0, 500, 2500 and 4500 G.

We see from this figure that the shape and nonlinearity of the plots remain basically unaltered by the magnetic field. In Figure 3 we show the magnetic field dependence of the output current with constant drain voltage kept at $V_d = +5$ V. The current changes by merely 2.4 mA for the magnetic field difference, $\Delta H = 3500$ G which amounts to an average increase of 0.7 $\mu A \cdot G^{-1}$. It is easy to visualize why the separation between the subsequent I-V plots keep on diminishing with increasing magnetic field in Figure 2.

The I-V characteristic at H=0 obeys a power law given by $I \propto V^{\alpha}$ where α is the nonlinear coefficient (NLC) of the varistor diode. It is also the measure of the figure-of-merit of the device. Larger values of the NLC lead to the better performance of the varistor. The value of NLC (α) is found to be 2.77 at H = 0 which reduces to 2.63 at H = 4500 G

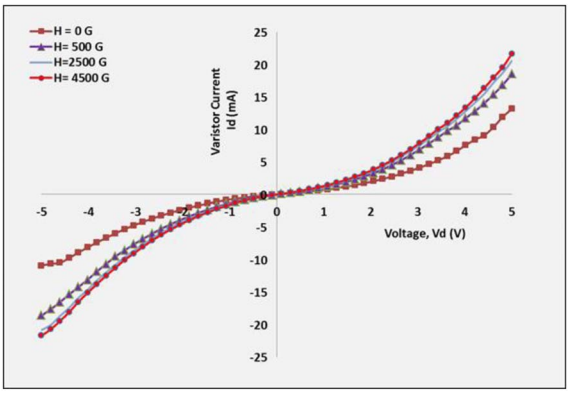

FIGURE 2. **Magnetic field dependence of current-voltage characteristics of an IHC 45 varistor at room temperature.**

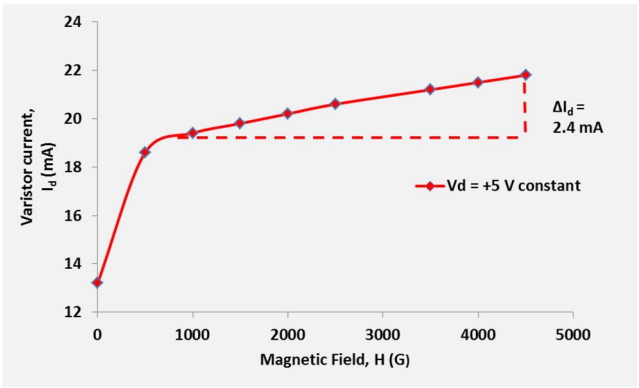

FIGURE 3. **Magnetic field dependence of the varistor output current with constant drain voltage at + 5V for an IHC 45 varistor.**

amounting to a reduction of just under 5%. This small loss in varistor's efficiency suggest that the device should perform satisfactorily as a varistor even in the presence of a magnetic field for circuit protection which is its traditional application.

When the varistor's I-V characteristics are plotted as resistance vs. voltage (R-V), the device gets the name of VDR which stands for *voltage dependent resistor*. VDR devices also have many applications in electronics. Recently it has been established that VDRs based on iron titanate substrates can perform satisfactorily as a magnetic field sensor in the range of 0<H<4500 G [13], [14]. Like its counterpart, a VDR device also obeys a power law which is given by $R \propto V^{-\beta}$. The NLC of varistor and VDR are obviously related and they satisfy the relationship: $\beta = (1 - \alpha)$.

Because of the magneto-resistive property of materials the varistor resistance would either increase or decrease according to the polarity of the magnetic field applied. This would naturally reflect in the respective values of the output currents (I_d) for H>0. The contributions to drain current (I_d) made by the applied magnetic field can be computed using equation (1).

$$I_d\,(T) = I_d \pm I_0 \tag{1}$$

where, I_0 is the initial unbiased current and $I_d(T)$ the magnetically contributed component to the drain current.

Alternatively, according to the convention followed in practice equation (1) can be rewritten as a set of two dependent equations.

$$+I_d\,(T) = I_d - I_0 \;\; when \;\; I_d > I_0 \tag{2a}$$

$$-I_d\,(T) = I_0 - I_d \;\; when \;\; I_0 > I_d \tag{2b}$$

The two output currents, I_d, with H>0 and I_0 with H=0 are experimentally determined whereas $I_d(T)$ must be extracted from I_d using equations 2(a) and 2(b). The resulting $I_d(T)$-V characteristics for the HFET transistor in its I-V mode have been plotted in Figure 4 for H= 500, 1500, 2500 and 4500 G.

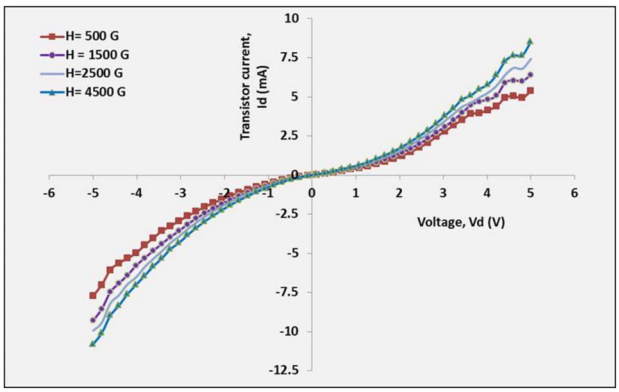

FIGURE 4. **Current-voltage plots as a function of varying magnetic fields of an IHC45 HFET transistor at room temperature.**

The transistor I-V characteristics are well developed and the output current increases with respect to the increasing magnetic field. The transistor output current appears to be about 30 % of the varistor current. This suggests that the contribution of the magnetic field to the varistor current is substantial and most of it happens up to H=1000G above which it is rather small because of the sample approaching saturation.

For both the varistor and its embedded transistor, we can determine the signal amplification and magnetic conduction coefficient (MCC) which is analogous to transconductance (also called mutual conductance) for a conventional transistor. Signal amplification and transconductance are the two signature properties of a transistor. Our results indicate that not only the embedded HFET rather also the magnetically tuned varistor acquires these properties which expand its range of applications. We define signal amplification (S_a) and MCC, $\mu(H)$ with the help of equations 3 and 4, respectively.

$$S_a = \left[\frac{\{I_d\,(T)_{at\ \max H}\}}{\{I_d\,(T)_{at\ \min H}\}} x100\right] \;\; with \;\; V_d \;\; constant \tag{3}$$

$$\mu(H) = \frac{I_d\,(T)\cdot V_d^{-1}}{H} \approx \frac{G\,(T)}{H} \approx \frac{\Delta G\,(T)}{\Delta H} \tag{4}$$

We can also find the current detectivity (I^*) of the device by defining it as $\frac{\Delta I_d(T)}{\Delta H}$ while keeping the drain voltage,

V_d, constant. These parameters are tabulated in Table 2 along with the potential applications for the magnetically tuned varistor and its embedded transistor.

TABLE 2. Properties of magnetically tuned varistor in I-V mode and its embedded transistor; MCC stands for magnetic conductance coefficient, μ(H).

Devices	Current detectivity, I* at V_d= +5 V ($A \cdot G^{-1}$)	MCC, μ(H) at V_d= +5 V ($\mu S \cdot G^{-1}$)	Maximum Amplification (%) at V_d = +5V	Nonlinear coefficient, (NLC), α	Potential Applications
Varistor	1.24×10^{-6}	25	140	2.77 at H=0 2.63 at H= 4500 G	Current and magnetic field detection; and circuit protection
Transistor	1.1×10^{-3}	2.11	380	None	Current detection and signal amplification.

The two parameters, I* and μ(H), can be considered as important parameters of the HFET transistor just as the current amplification and transconductance are the defining properties of conventional semiconductor transistors. In spite of the fact that the I-V characteristics of the HFET transistor does not display saturated regions we can make use of this device as a current detector and signal amplifier.

B. EXPERIMENT 2: MAGNETIC FIELD DEPENDENCE OF V-I CHARACTERISTICS OF AN IHC 45 VARISTOR AT ROOM TEMPERATURE

For this experiment a current was injected between the S and D contacts and the resulting voltage monitored while varying the H-field. This yields the varistor V-I characteristics as seen from Figure 5. The individual plots are almost impossible to distinguish from each other because the output voltage, V_d, changes by merely 58 mV for 0<H<-4000 G and as such it simply remains buried in the scale used. However, the picture changes drastically after the magnetic field induced changes in the output voltage are determined.

In Figure 5 the individual V-I plots display pronounced nonlinearity similar to the nonlinearity found for the corresponding I-V plots (Figure 2). The V-I plots follow a power law described by $V \propto I^{\gamma}$ where γ is the NLC of the V-I varistor. Its value is 0.53 when H=0 and it reduces to 0.49 when H= -4000 Oe. This is a change of about 7% indicating that magnetic fields do not affect the varistor diode to hinder its capacity to be used for protecting electronic components and circuits from abrupt current fluctuations. Normally the V-I mode of a varistor is used for avoiding damage to a circuit and its components because of fluctuations in the supply current.

In order to determine the contributions of the applied magnetic fields to the output voltage, V_d, we can take the same approach as we did for the case of the HFET in its I-V mode (see equations 2(a) and 2(b). Let us assume that each V_d corresponding to H>0 consists of two components; one being the initial signal, V_0 with H =0 and the other

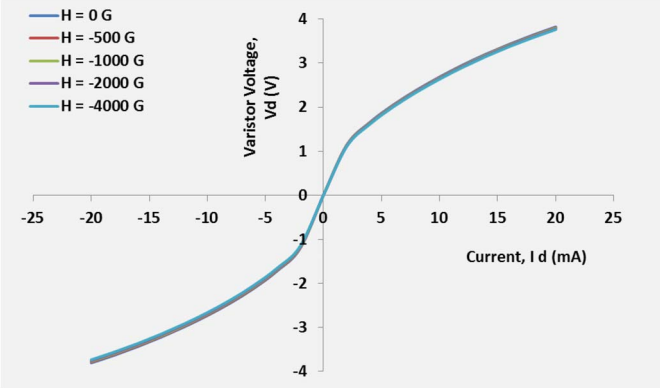

FIGURE 5. Voltage vs. current plots of IHC 45 varistor with varying magnetic fields at room temperature.

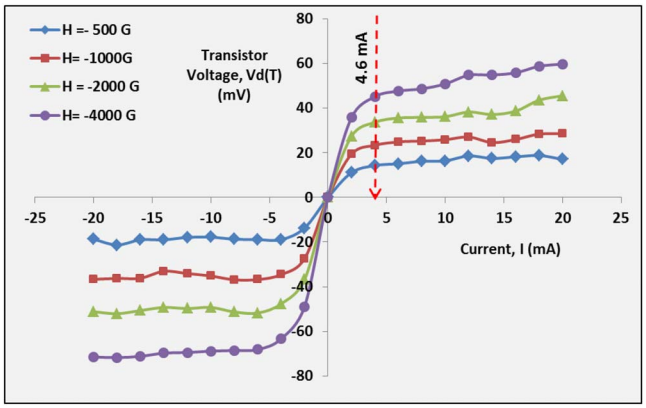

FIGURE 6. Voltage - current plots with varying magnetic fields of an IHC45 HFET transistor at room temperature.

V_d(T) with H>0. For evaluation of the hidden signal V_d(T) we make use of Equation (5) which states that:

$$V_d(T) = V_d \pm V_0 \tag{5}$$

The polarity of V_d(T) will depend upon whether V_d is greater or smaller than V_0. This leads us to the two components of equation (5).

$$+V_d(T) = (V_d - V_0) \quad when \quad V_d > V_0 \tag{6a}$$

$$-V_d(T) = (V_0 - V_d) \quad when \quad V_d < V_0 \tag{6b}$$

The V_d(T)-I characteristics for the embedded device are plotted in Figure 6. It should be noted that the magnetic contributions, that is V_d(T), are in mV range which is three orders of magnitude smaller than that of varistor output, V_d. Here the individual plots are easily distinguishable with a good level of separation between each other.

Contrary to the HFET device in its I-V mode (see Figure 4) here each individual V-I curve attains saturation in both the forward and reverse mode of the device. The transition of each plot from the negative current side to the positive current side passes smoothly through the origin. Initially the output voltage increases linearly with increasing current and then begins to reach saturation above the switching current

TABLE 3. Properties and potential applications of magnetically embedded HFET transistors; MRC stands for magnetic resistance coefficient. Its symbol is η(H).

Room Temperature	Constant current, I_d (mA)	Voltage detectivity, V* ($\mu V \cdot G^{-1}$)	MRC, η(H) ($\mu\Omega \cdot G^{-1}$)	Maximum amplification, S_a (%)	Potential Applications
+H	+20	50.9	206	830	Good voltage amplifier
+H	-20	76.9	227	1260	Good voltage amplifier
-H	+20	12.2	610	350	Voltage amplifier; excellent magnetic field detector and voltage sensor
-H	-20	15.1	12.2	380	Voltage amplifier, voltage and resistance sensor
Temperature: 100 K	Constant Current, I_d (μA)	V* detectivity ($(\mu V \cdot G^{-1})$)	MRC, η(H) ($\mu\Omega \cdot G^{-1}$)	Maximum Amplification (%)	Potential Applications
+H	+2	46.5	1.57	3500	Excellent resistance sensor and excellent voltage amplifier
+H	-2	102	0.56	2800	Excellent resistance sensor and excellent voltage amplifier

of 4.6 mA. Simply by biasing the device with 4.6 mA the HFET transistor can be used as an "off" and "on" switch. The saturated characteristics of the output signal and the feature of electronic switching are the two important attributes that make the HFET transistor in its V-I mode a good candidate for being recognized in the family of magnetic transistors. Furthermore we find that the device is also capable of providing a good level of amplification of the output signal. It can be as high as 380%. However, if the same device is subjected to positive magnetic fields the signal amplification can reach as high as 1260%.

The signal amplification (S_a) and transresistance coefficient (MRC) for this device were evaluated by slightly modifying equations (3) and (4), respectively. The voltage detectivity (V*) was found by determining the ratio $\frac{\Delta V_d(T)}{\Delta H}$ while keeping the drain current, I_d, constant. In Table 3 the typical device parameters and potential applications for this HFET is summarized. This table also includes these parameters for the magnetically induced HFET transistor tuned by +H-fields though we have not shown the actual plots here. No qualitative difference could be found distinguishing the HFET characteristics whether the modifying agent is a +H-field or −H –field. The V-I plots display similar traits.

C. EXPERIMENT 3: MAGNETIC FIELD DEPENDENCE OF V-I CHARACTERISTICS OF AN IHC 45 VARISTOR AT 100K

The device, when cooled to 100K, shows a robust response to applied magnetic fields as can be seen from Figure 7. It is well known that the magnetic moment of a ferromagnetic material increases at low temperatures. At the same time the resistance of a semiconductor material also increases exponentially when cooled. IHC45 being simultaneously

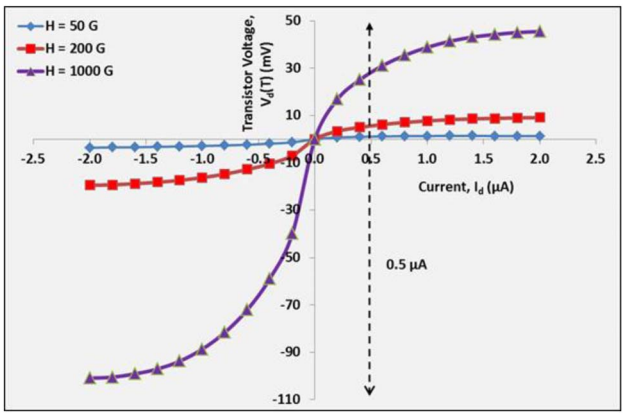

FIGURE 7. Voltage - current plots with varying magnetic fields of an IHC45 HFET at 100 K.

a ferromagnetic and a semiconductor material would obviously exhibit the effect of low temperatures in its magnetic and electronic properties. Therefore we can identify some interesting features of Figure 7. First the current applied for the device at 100 K is in μA range which is about three orders of magnitude smaller than the currents applied for the same device at room temperature. Yet the voltage output is of the same order as for the room temperature device, both being in mV range. Secondly, each plot is bipolar with well-developed nonlinearity and saturated regions. Thirdly the signal amplification is impressive; it is greater by many-folds than what it is at room temperature. As indicated in the figure the switching current for this device appears to be approximately 0.5 μA. Values for relevant parameters along with potential applications for this low temperature device are also included in Table 3. All these devices also appear

to be good voltage detectors because of their sensitivity equivalent to $46.5<V^*<102$ μV per Gauss.

V. CONCLUSION

The paper outlines the fabrication, properties and potential applications of magnetic field effect transistor (HFET) devices which are produced under three experimental conditions: (a) first, by subjecting the current-voltage characteristics of a varistor diode to varying magnetic fields (HFET in I-V mode); (b) second, by studying the effect of applied magnetic fields on the voltage-current characteristics of the same varistor diode (HFET in V-I mode); and (c) thirdly, repeating the same experiments by cooling the varistor sample to 100 K (low temperature HFET in V-I mode). Experimentally determined values of various parameters along with the potential applications of the HFET transistors have been summarized in Tables 2 and 3. The device when cooled to 100 K becomes an excellent signal amplifier whereas the room temperature HFET transistor is endowed with other excellent transistor properties. The HFET is a very simple device which is embedded in a varistor diode and is based on the concept of easy to produce with good reliability and precision. Its fundamental mechanism is based on simple physics. In contrast the other two magnetic transistors are highly sophisticated devices; one being the spin mediated device and the other based on the principles of magnetic valve. Their platforms require sophisticated level of skill to produce and operate. In contrast to conventional semiconductor transistors the HFET devices are built on ceramic substrates for which the processing is straight forward and simple and can be produced in large volumes rather inexpensively. We presume that because of the materials properties inherent to the IHC45 magnetic oxide semiconductor the HFET devices should perform well also under hazardous conditions such as at high temperature and radiation dominant environments. Being based on ceramic substrates they are expected to be rugged and capable of withstanding abuses commonly encountered under field conditions.

ACKNOWLEDGMENT

Special thanks of authors go to Dr. P. Padmini (deceased), Dr. Jian Dou, both of the University of Alabama at Tuscaloosa, AL; and to their former students Mr. Ivan Sutanto and Ms. Amanda A. Scantlin of Ingram School of Engineering at Texas State University at San Marcos, TX for sharing their data with them.

REFERENCES

[1] K. Dawson, "Electric field controlled semiconductor device," U.S. Patent 3 102 230, Aug. 27, 1963.
[2] R. C. Gallagher and W. S. Corak, "A metal-oxide-semiconductor (MOS) Hall element," *Solid State Electron.*, vol. 9, no. 5, pp. 571–580, 1966.
[3] G. R. M. Rao and W. N. Carr, "Magnetic sensitivity of a MAGFET of uniform channel current density," *Solid State Electron.*, vol. 14, no. 10, pp. 995–1001, 1971.
[4] S. Datta and B. Das, "Electronic analog of the electro-optic modulator," *Appl. Phys. Lett*., vol. 56, no. 7, pp. 665–667, 1990. [Online]. Available: http://dx.doi.org/10.1063/1.102730
[5] D. J. Monsma, J. C. Lodder, T. J. Popma, and B. Dieny, "Perpendicular hot electron spin-valve effect in a new magnetic field sensor: The spin-valve transistor," *Phys. Rev. Lett.*, vol. 74, no. 26, pp. 5260–5263, 1995.
[6] Y. Ishikawa, "Magnetic properties of the $FeTiO_3$-Fe_2O_3 solid solution series," *J. Phys. Soc. Jpn.*, vol. 12, no. 10, pp. 1083–1098, 1957.
[7] Y. Ishikawa, "Electrical properties of FeTiO3-FeeO3 solid solution series," *J. Phys. Soc. Jpn.*, vol. 13, no. 1, pp. 37–42, 1958.
[8] L. Navarrete *et al.*, "Magnetization and curie temperature of ilmenite-hematite ceramics," *J. Amer. Ceram. Soc*., vol. 89, no. 5, pp. 1601–1604, 2006.
[9] M. R. Cássia-Santos *et al.*, "Recent research developments in SnO_2-based varistors," *Mater. Chem. Phys.*, vol. 90, no. 1, pp. 1–9, 2005.
[10] C.-W. Nahm, "Electrical properties and dielectric characteristics CCT-doped Zn/Pr-based varistor with sintering temperature," *Trans. Elect. Electron. Mater*. vol. 10, no. 3, pp. 80–84, 2009.
[11] R. K. Pandey, W. A. Stapleton, P. Padmini, J. Dou, and R. Schad, "Magnetically tuned varistor-transistor hybrid device," *AIP Adv.*, vol. 2, no. 4, pp. 1–8, 2012, doi: 10.1063/1.4773328.
[12] C. Lohn *et al.*, "IV and CV characteristics of multifunctional ilmenite-hematite $0.67FeTiO_3$–$0.33Fe_2O_3$," in *Functionalized Nanoscale Materials, Devices and Systems* (NATO Science for Peace and Security Series B: Physics and Biophysics). Dordrecht, The Netherlands: Springer, 2008, pp. 419–424.
[13] R. K. Pandey, W. A. Stapleton, and I. Sutanto, "Voltage biased magnetic sensors based on IHC 45 VDRs," in *Proc. Process. Properties Adv. Ceramics Composites VII*, vol. 252. 2015, pp. 115–130.
[14] R. K. Pandey, W. A. Stapleton, I. Sutanto, and M. Shamsuzzoha, "Voltage-biased magnetic sensors based on tuned varistors," *J. Electron. Mater.*, vol. 44, no. 4, pp. 1100–1109, 2015, doi: 10.1007/s1664-015-3632-9.

RAGHVENDRA K. PANDEY is an Ingram Professor of Electrical Engineering with the Ingram School of Engineering, Texas State University, San Marcos, TX, USA. He has been in academia for over 40 years. Before joining the faculty at Texas State University, in 2008, he was with the University of Alabama, Tuscaloosa, AL, USA, from 1997 to 2007. He was with Texas A&M University, for 20 years. He has published extensively in national and international scientific journals, holds ten U.S. patents, and presented invited lectures and seminars. He has made valuable contributions in the fields of electronic materials, ferroelectricity, magnetism, high temperature superconductors, and MEMS. For the past five years he has been researching mainly in electroceramic materials and devices. He was a recipient of many honors and multiple teaching and research awards. He is a fellow of the American Ceramic Society.

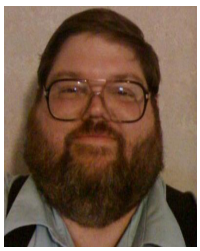

WILLIAM A. STAPLETON received the Ph.D. degree in electrical engineering from the University of Alabama, in 1997. He is currently an Associate Professor of Electrical Engineering with Texas State University, San Marcos, TX, USA. His formal specializations encompass analog and digital electronics, computer architecture, distributed computing, and embedded computing. His avocations also include electric vehicles and solar energy applications. He is a member of the IEEE society.

RAINER SCHAD received the M.Sc. and Ph.D. degrees in physics from Leibniz University, Hannover, Germany, in 1987 and 1991, respectively. In 1992, he joined the Solid State Physics Group, Catholic University of Louvain, Belgium, as a Post-Doctoral Fellow. From 1995 to 1998, he was a Post-Doctoral Fellow with the Catholic University of Nijmegen, The Netherlands. In 1998, he joined the Department of Physics and Astronomy, University of Alabama, Tuscaloosa, USA, as an Assistant Professor. He currently holds the rank of Professor. He specializes in structural, electric, and magnetic properties of thin films.